Carbohydrate Polymers 114 (2014) 521–529

Contents lists available at ScienceDirect

Carbohydrate Polymers

journal homepage: www.elsevier.com/locate/carbpol

Simultaneous removal of Co(II) and 1-naphthol by core–shell structured Fe_3O_4@cyclodextrin magnetic nanoparticles

Xiaobao Zhang [a,b,1], Yong Wang [b,1], Shitong Yang [b,*,1]

[a] Department of Polymer Science and Engineering, College of Chemistry, Chemical Engineering and Materials Science, Soochow University, 215123 Suzhou, PR China

[b] School for Radiological and Interdisciplinary Sciences, Soochow University, 215123 Suzhou, PR China

ARTICLE INFO

Article history:
Received 20 April 2014
Received in revised form 19 July 2014
Accepted 13 August 2014
Available online 2 September 2014

Keywords:
Fe_3O_4@CD MNPs
Co(II)
1-Naphthol
Simulated effluent
Magnetic separation

ABSTRACT

Herein, β-cyclodextrin (β-CD) was introduced on the surfaces of Fe_3O_4 particles via the chemical co-precipitation approach. The as-prepared Fe_3O_4@CD MNPs can be easily separated from the aqueous phase with a magnet. The removal performance of Fe_3O_4@CD MNPs toward Co(II) and 1-naphthol were investigated by using the batch technique. The maximum sorption capacities of Fe_3O_4@CD MNPs toward Co(II) and 1-naphthol are higher than a series of adsorbent materials. The simultaneous removal of Co(II) and 1-naphthol is achieved via the binding of Co(II) on the external surface sites of Fe_3O_4@CD MNPs and the incorporation of 1-naphthol into the hydrophobic cavity of surface-coated β-CD. The Fe_3O_4@CD MNPs exhibit favorable removal performance toward Co(II) and 1-naphthol from the simulated effluent. The experimental results herein suggest that Fe_3O_4@CD MNPs can be used as cost-effective material for the purification of co-contaminated water systems.

1. Introduction

With the rapid development of industrial and agricultural production processes, various heavy metal ions and organic contaminants are discharged into the natural environment. Cobalt (Co(II)) is commonly present in effluents due to its widely application in mechanotronics, galvanization, alloy materials, batteries manufacturing, pigment processing, catalyst production, medical diagnosis, and etc. The ionizable aromatic compounds (e.g., naphthol and naphthylamine) are widely present in the wastewaters discharged from pesticides, dyestuffs, pharmaceuticals, petrochemicals, and etc. The high toxicity and harmful effects of these pollutants on ecosystem and human heath have aroused widespread concern all over the world (Liu et al., 2003; Wang et al., 2010). In view of this, the significant environmental priority nowadays is to exploit advanced techniques and adsorbent materials for the effective remediation of co-contaminated soil and water systems.

Among the current techniques for environmental remediation, the sorption approach has been extensively used due to a series of advantages such as simple device, easy operation, high security, high efficiency, low cost and no secondary pollution. A series of adsorbent materials such as bentonite, fly ash, activated bamboo charcoal, carbon nanotubes, glycine-β-cyclodextrin and so on have been tested for the simultaneous removal of inorganic and organic pollutants (Diaz-Flores, López-Urías, Terrones, & Rangel-Mendez, 2009; Jović-Jovičić et al., 2010; Ma, Wang, Huang, & Wang, 2010; Visa, Bogatu, & Duta, 2010; Wang et al., 2010). However, the difficulty for separating these materials from the aqueous phase limits their application potential in effluent purification. Recently, some magnetic composites with high separation convenience have been exploited to compensate for this deficiency (Chen et al., 2012a; Chen, Zhang, Wang, Li, & Guo, 2012b; Shen, Pan, Zhang, Huang, & Gong, 2012; Singh, Barick, & Bahadur, 2013; Zhu et al., 2011). For instance, Chen et al. (2012a) prepared a thiourea-modified ion-imprinted chitosan/TiO_2 (MICT) composite for the simultaneous removal of Cd(II) and 2,4-dichlorophenol. The experimental results showed that the MICT composite exhibited a maximum sorption capacity of 256.41 mg/g toward Cd(II) and a degradation efficiency of 98% toward 2,4-dichlorophenol. Singh et al. (2013) reported that the prepared Fe_3O_4 embedded ZnO nanocomposites (Fe_3O_4–ZnO MSN) via a facile soft-chemical approach showed strong tendency for the simultaneous removal of Co(II), Pb(II), Hg(II) and As(III) from wastewater. In addition, the Fe_3O_4–ZnO MSN exhibited high photocatalytic activity for degradating organic dyes (rhodamine B, methyl orange and methylene blue) and also high efficiency for

* Corresponding author. Tel.: +86 512 65883945; fax: +86 512 65883945.
E-mail address: shitongyang@suda.edu.cn (S. Yang).
[1] Collaborative Innovation Center of Radiation Medicine of Jiangsu Higher Education Institutions.

http://dx.doi.org/10.1016/j.carbpol.2014.08.072
0144-8617/

capturing bacteria pathogens. From the forgoing literatures, one can conclude that magnetic composites exhibit favorable performance for the simultaneous removal of toxic heavy metal ions and organic contaminants from aquatic systems.

Cyclodextrin (CD) is a kind of torus-shaped cyclic oligosaccharide containing several α-1,4-linked D-glucopyranose units with an internal hydrophobic cavity. CD possesses an excellent capacity to form inclusion complexes with properly sized and structured organic molecules through host–guest interactions. The three types of natural CDs (i.e., α-CD, β-CD and γ-CD) and their derivatives (e.g., the randomly methylated-β-CD (RMβCD), hydroxypropylated-α-CD (HPαCD), hydroxypropylated-β-CD (HPβCD), hydroxypropylated-γ-CD (HPγCD) and sulfobutyl ether-β-CD (SBEβCD)) have been produced and used in food, cosmetics, catalysis, molecular recognition, drug delivery and environmental protection fields (Badruddoza, Tay, Tan, Hidajat, & Uddin, 2011; Chen, & Liu, 2010; del Valle, 2004; Fuhrer, Herrmann, Athanassiou, Grass, & Stark, 2011; Loftsson, & Brewster, 2011; Maturi, & Reddy, 2006; Morin-Crini, & Crini, 2013). Among these CD products, β-CD is the most accessible, the lowest-priced and generally the most useful type (del Valle, 2004). Compared with the α-CD and γ-CD, the β-CD shows much better capacity for the removal of phenol from water due to the optimal size matching (Chen et al., 2012b). In view of this, β-CD was selected and introduced on Fe_3O_4 magnetic nanoparticles (MNPs) via the chemical co-precipitation approach to prepare core–shell structured Fe_3O_4@CD MNPs. Herein, the use of natural CD instead of the derivatives can simplify the synthetic procedures and reduce the preparation cost of Fe_3O_4@CD MNPs. The properties of bare Fe_3O_4 and Fe_3O_4@CD MNPs were characterized by using the Fourier transform infrared spectroscopy (FTIR), X-ray diffraction (XRD), transmission electron microscopy (TEM), elemental analysis and magnetization curves. Afterward, batch experiments were conducted to evaluate the removal performance of Fe_3O_4@CD MNPs toward Co(II) and 1-naphthol. The application potential of Fe_3O_4@CD MNPs for effluent purification was further evaluated on the basis of the experimental results.

2. Experimental details

2.1. Materials and reagents

The β-cyclodextrin (β-CD), $CoCl_2{\cdot}6H_2O$, $FeCl_2{\cdot}4H_2O$ and $FeCl_3{\cdot}6H_2O$ chemicals were purchased from Sinopharm Chemical Reagent Co. Ltd. (China). The analytical pure $CoCl_2{\cdot}6H_2O$ was dissolved in deionized water to obtain the Co(II) stock solution in a concentration of 200 mg/L. The prepared Co(II) stock solution were diluted to the required concentrations in the following experiments. The 1-naphthol powders were dissolved in a solution (pH ~6.5) containing 100 mg/L NaN_3 to prepare the 1-naphthol stock solution. Herein, the NaN_3 was used as a biocide to prevent the biodegradation of 1-naphthol (Oleszczuk, Pan, & Xing, 2009; Wang, Tao, & Xing, 2009b). In order to ensure complete dissolution, the 1-naphthol concentration was restricted to below 50% of its water solubility.

2.2. Preparation and characterization

The bare Fe_3O_4 and Fe_3O_4@CD MNPs were prepared by using the chemical co-precipitation method. First, 10 g of $FeCl_2{\cdot}4H_2O$ and 14.5 g of $FeCl_3{\cdot}6H_2O$ were dissolved in 200 mL Milli-Q water and heated to 90 °C. Afterward, 40 mL of ammonium hydroxide (25%) solution and 100 mL of NaCl solution containing 1.2 g of β-CD were rapidly and sequentially added into the vessel. The mixture was vigorous stirred under nitrogen atmosphere for 50 min and then cooled to room temperature. The Fe_3O_4@CD precipitates were collected by using an external magnet. Afterward, the wet pastes were washed several times with ethanol and Milli-Q water and then dried in vacuum oven. The control sample of bare Fe_3O_4 was synthesized in the similar way without the addition of β-CD. The zero point charge (pH_{zpc}) values of bare Fe_3O_4 and Fe_3O_4@CD MNPs are identified to be ~6.8 and ~4.0, respectively. Herein, the lower pH_{zpc} value of Fe_3O_4@CD MNPs suggests that β-CD has been successfully grafted on the Fe_3O_4 surfaces. According to the N_2-BET method, the specific surface area of bare Fe_3O_4 and Fe_3O_4@CD MNPs were measured to be 18.5 and 26.4 m^2/g, respectively. The FTIR spectra were collected and analyzed to identify the binding mechanism for the formation of Fe_3O_4@CD MNPs. The XRD patterns were recorded on a MAC Science Co. M18XHF diffractometer using Cu $K\alpha$ radiation. TEM images were performed on JEOL-2010 microscope to characterize the morphology and size distribution of bare Fe_3O_4 and Fe_3O_4@CD MNPs. The magnetic measurements were performed in a MPMS-XL SQUID magnetometer.

2.3. Experimental procedure

The sorption experiments were performed by using the batch technique in amber EPA vials equipped with Teflon-lined screw caps. Briefly, the adsorbent suspensions, NaCl electrolyte solution, Co(II) and 1-naphthol stock solutions were added to achieve the required concentrations of individual components. The pH values were adjusted to desired values by adding tiny amounts of HCl or NaOH solutions. The obtained mixtures were gently oscillated for 24 h to achieve sorption equilibrium. Afterward, a permanent magnet was used to separate the solid from the liquid phases. The concentration of Co(II) in the supernatants was measured by using the atomic absorption spectroscopy. The concentration of 1-naphthol was measured by using the UV–vis spectrophotometer at 332 nm. To improve the determination sensitivity, the supernatants were basified with 0.1 mol/L NaOH solution to achieve the dissociation state of 1-naphthol. The sorption percentage ($S\% = (C_0 - C_e)/C_0 \times 100\%$), sorption amount ($q_e = (C_0 - C_e)V/m$) and the distribution coefficient ($K_d = q_e/C_e \times 100\%$) of Co(II) and 1-naphthol were calculated from the initial concentration (C_0), the final concentration (C_e), the adsorbent mass (m) and the suspension volume (V).

3. Results and discussion

3.1. Characterization

Fig. S1 shows the FTIR spectra of bare Fe_3O_4, Fe_3O_4@CD MNPs and pure β-CD. For bare Fe_3O_4 (curve A), the peak at 586 cm^{-1} corresponds to the stretching vibration of Fe—O bond. For Fe_3O_4@CD MNPs (curve B), the characteristic peak of the Fe—O bond slightly shifts to ~580 cm^{-1}. This variation trend suggests that the Fe—O bond is involved in the formation of Fe_3O_4@CD MNPs. The spectrum of Fe_3O_4@CD MNPs (curve B) shows all the characteristic peaks of pure β-CD (curve C) with a slight shift. This phenomenon suggests that the β-CD moieties have been successfully grafted on the Fe_3O_4 surfaces. Based on the foregoing analysis, the Fe_3O_4@CD MNPs are formed via the interaction between the functional groups of β-CD and the Fe—O bond of the Fe_3O_4 cores. As shown in Fig. S2, the XRD pattern of Fe_3O_4@CD MNPs is similar to that of bare Fe_3O_4. This phenomenon indicates that the surface coating of β-CD does not alter the cubic phase of the Fe_3O_4 cores. Detailed discussions on the FTIR spectra and XRD patterns are described in the Supporting information. Fig. S3A and B shows the TEM images of bare Fe_3O_4 and Fe_3O_4@CD MNPs, respectively. It is clear that the bare Fe_3O_4 particles form a mass of agglomeration, exhibiting

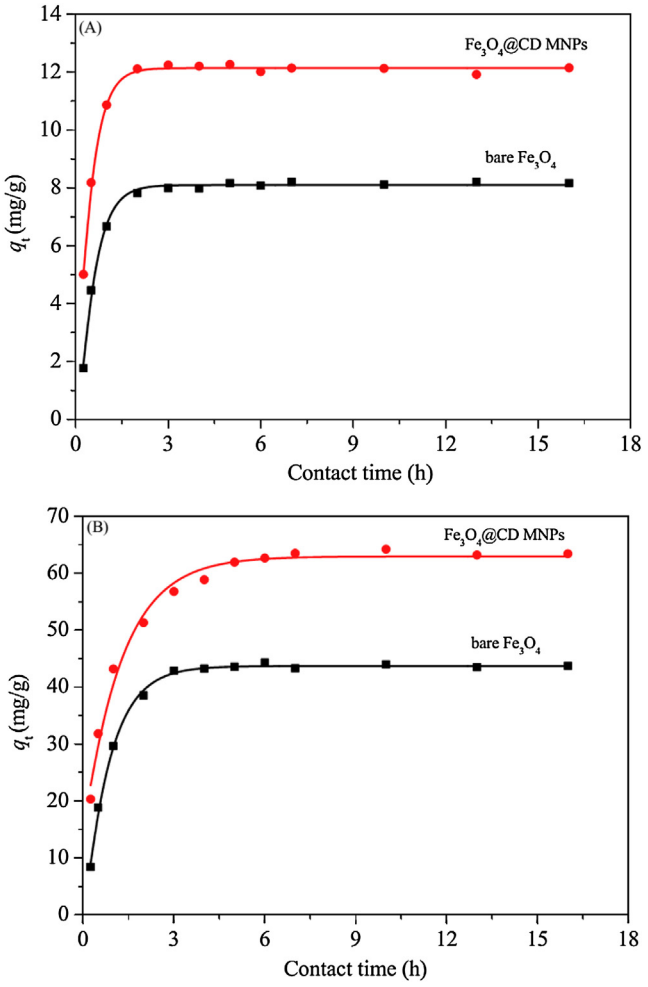

Fig. 1. Sorption kinetics of Co(II) (A) and 1-naphthol (B) on bare Fe_3O_4 and Fe_3O_4@CD MNPs. T = 293 K, pH = 6.5, m/V = 0.5 g/L, $C_{Co(II)}$ = 10 mg/L, $C_{1\text{-naphthol}}$ = 50 mg/L, I = 0.01 mol/L NaCl.

no uniform shape and size. In contrast, the Fe_3O_4@CD MNPs disperse uniformly in quasi-spherical shape with an average size of ~200 nm. The obvious differences suggest that the surface-coated β-CD moieties greatly enhance the dispersion of Fe_3O_4@CD MNPs in solution. Elemental analysis suggests that the grafted amount of β-CD on the Fe_3O_4 cores is 115 mg/g (i.e., 11.5% in w/w). In addition, the grafted amount of natural organic matter on the solid surfaces can be quantitatively verified from the magnetization curves (Liu, Zhao, & Jiang, 2008; Yang, Zong, Ren, Wang, & Wang, 2012). As shown in Fig. S4, the saturation magnetization (M_s) of bare Fe_3O_4 and Fe_3O_4@CD MNPs are 77.1 and 67.9 emu/g, respectively. The decreased M_s value of 9.2 emu/g corresponds to a grafted β-CD content of ~11.9% (w/w), which agrees well with that calculated from the elemental analysis (11.5% in w/w). Undoubtedly, the M_s value of Fe_3O_4@CD MNPs is high enough for their separation from the liquid phase by using a magnet (inset in Fig. S4).

3.2. Single-solute sorption systems

3.2.1. Effect of contact time

Fig. 1A shows the sorption kinetics data of Co(II) on bare Fe_3O_4 and Fe_3O_4@CD MNPs. One can see that the sorption amount increases rapidly in the initial contact time of 2 h, and then keeps almost unchanged after 2 h. Note that the transitory time for separating bare Fe_3O_4 and Fe_3O_4@CD MNPs from the aqueous solution with an external magnet is ignored when calculating the total contact time. Herein, such a short time for reaching sorption equilibrium suggests the occurrence of chemical complexation rather than physical sorption (Wang, Dong, He, Chen, & Yu, 2009a). Specifically, the fast sorption kinetics procedure is attributed to the rapid migration of Co(II) from the solution onto the external sites of bare Fe_3O_4 and Fe_3O_4@CD MNPs.

Fig. 1B illustrates the sorption kinetics data of 1-naphthol on bare Fe_3O_4 and Fe_3O_4@CD MNPs. It is interesting to find that 1-naphthol exhibits distinct sorption trends on the two materials. Specifically, the sorption of 1-naphthol on bare Fe_3O_4 increases rapidly with increasing contact time and reaches equilibrium after 3 h. Herein, the unrestricted transport of 1-naphthol from the solution onto the surfaces of bare Fe_3O_4 without diffusion resistance is the acceptable interpretation for the observed sorption kinetics trend (Zhang, Niu, Cai, Zhao, & Shi, 2010). In contrast, the sorption kinetics of 1-naphthol on Fe_3O_4@CD MNPs contains two successive procedures, i.e., an initial fast rate followed by a subsequent slow rate. The sorption process reaches equilibrium after a contact time of ~7 h. It is necessary to interpret the sorption trend of 1-naphthol based on the structural configuration of Fe_3O_4@CD MNPs. The surface-coated β-CD molecules possess a characteristic truncated-cone structure with hydrophilic hydroxyl sites on the external surfaces and hydrophobic cylindrical cavity in the interior (Badruddoza et al., 2011). During the initial stage of contact time, 1-naphthol molecules tend to transfer rapidly from the solution onto the external surfaces of Fe_3O_4@CD MNPs. With time going on, the surface-attached 1-naphthol molecules gradually migrate into the internal cavity due to the hydrophobic interaction, forming strong inclusion complexes. Such slow diffusion will result in a slow increase in the sorption amount at the later kinetics stage (Al-Qunaibit, Mekhemer, & Zaghloul, 2005; Bhattacharyya & Gupta, 2008).

The required contact time to reach sorption equilibrium is significant for assessing the application potential of an adsorbent material in wastewater purification. Herein, the short sorption kinetics procedure suggests that Fe_3O_4@CD MNPs can be potentially used for continuous effluent purification. After reaching the sorption equilibrium, the pollutant-loaded Fe_3O_4@CD MNPs can be easily recovered by using an external magnet and subsequently regenerated for cyclic utilization. According to the sorption kinetics data, a shaking time of 24 h is chosen in the following experiments to ensure complete sorption equilibrium of Co(II) and 1-naphthol on Fe_3O_4@CD MNPs.

As shown in Fig. 1, the sorption amounts of Co(II) and 1-naphthol on Fe_3O_4@CD MNPs are higher than those on bare Fe_3O_4. Owing to the surface coating of β-CD moieties, the specific surface area of Fe_3O_4@CD MNPs (26.4 m^2/g) is higher than that of bare Fe_3O_4 (18.5 m^2/g). The surface-coated β-CD moieties contribute to the higher sorption performance of Fe_3O_4@CD MNPs toward Co(II) and 1-naphthol. The TEM images suggest that β-CD coating can efficiently reduce the aggregation of Fe_3O_4 MNPs in solution (Fig. S3B). Meanwhile, the surface-coated β-CD can also improve the physiochemical stability of Fe_3O_4 MNPs in solution. The enhanced dispersion and stability of Fe_3O_4@CD MNPs can improve the availability of surface hydroxyl sites and the cylindrical cavity for binding Co(II) and 1-naphthol.

3.2.2. Effect of pH

Fig. 2 shows the sorption percentage of Co(II) on Fe_3O_4@CD MNPs as a function of pH in 0.01 mol/L NaCl electrolyte solution. It is clear that solution pH plays a significant role in Co(II) sorption procedure. As shown in Fig. 2, the sorption of Co(II) increases slowly from ~20% to ~25% as pH increases from 2.0 to 4.0, then increases sharply from ~25% to ~98% as pH increases from 4.0 to 8.0, and finally maintains high level at higher pH range. Herein, the observed sorption trend can be interpreted by the relative

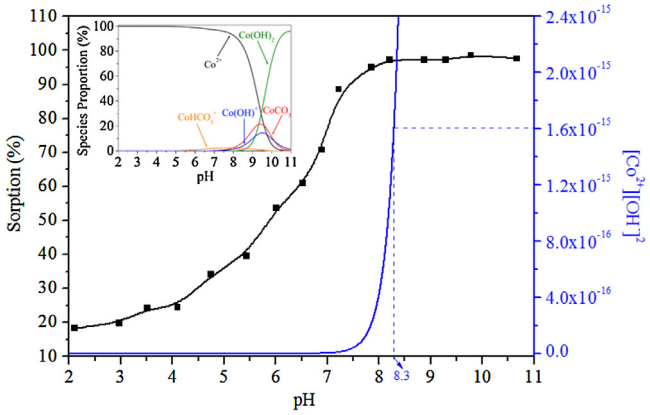

Fig. 2. Sorption of Co(II) on Fe_3O_4@CD MNPs as a function of solution pH. Inset: Relative proportion of Co(II) species in solution. T = 293 K, m/V = 0.5 g/L, $C_{Co(II)}$ = 10 mg/L, I = 0.01 mol/L NaCl.

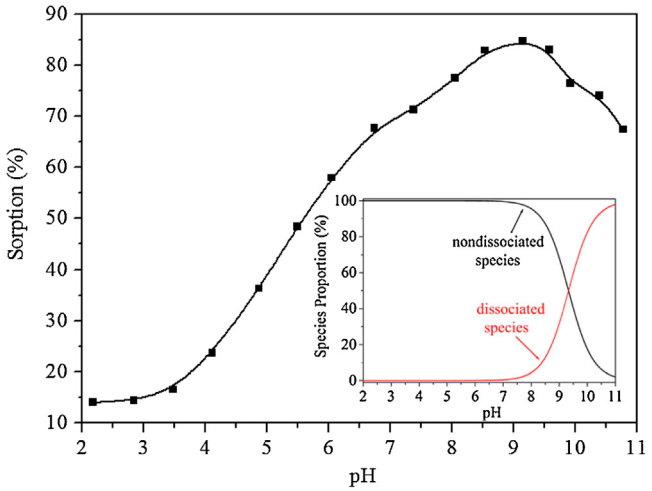

Fig. 3. Sorption of 1-naphthol on Fe_3O_4@CD MNPs as a function of solution pH. Inset: Relative proportion of 1-naphthol species in solution. T = 293 K, m/V = 0.5 g/L, $C_{1\text{-naphthol}}$ = 50 mg/L, I = 0.01 mol/L NaCl.

distribution of Co(II) species in solution and the surface properties of Fe_3O_4@CD MNPs in terms of surface charge and dissociation of functional groups. The inset in Fig. 2 illustrates the relative proportion of Co(II) species in solution as computed by Visual MINTEQ ver. 3.0 (Gustafsson, 2011). It is clear that Co(II) in solution is mainly present as the positively charged Co^{2+} species in the pH range of 2.0–8.0. The surfaces of Fe_3O_4@CD MNPs are positively charged below the pH_{zpc} value of ~4.0. The electrostatic repulsion between Co^{2+} ions and the protonated sites (i.e., SOH_2^+) on Fe_3O_4@CD surfaces results in the low Co(II) sorption percentage in the pH range of 2.0–4.0. In contrast, the surfaces of Fe_3O_4@CD MNPs become negatively charged at pH > 4.0 due to the deprotonation reaction (i.e., $SOH - H^+ \Leftrightarrow SO^-$). The electrostatic attraction between the negatively charged binding sites on Fe_3O_4@CD surface and the positively charged Co^{2+} species enhances the formation of strong complexes. In addition, the deprotonated surface sites can improve the dispersion of Fe_3O_4@CD MNPs in solution. This phenomenon will increase the contact area between Co^{2+} ions and the binding sites on Fe_3O_4@CD surfaces, which consequently enhances the sorption percentage of Co(II) at pH 4.0–8.0. The precipitation curve is illustrated to check whether the formation of hydroxide precipitates contributes to Co(II) sorption trend. One can see that Co(II) in solution begins to form $Co(OH)_2$(s) precipitates at pH ~8.3 (Fig. 2). Therefore, the abrupt increase of Co(II) sorption on Fe_3O_4@CD MNPs at pH < 8.0 is not attributed to the formation of $Co(OH)_2$(s) precipitates. At pH > 8.0, Co(II) is mainly present as $Co(OH)_2$ species with a proportion of $CoCO_3$ and $Co(OH)^+$ species in solution (inset in Fig. 2). Hence, the high sorption percentage of Co(II) on Fe_3O_4@CD MNPs at pH > 8.0 is attributed to the formation of $Co(OH)_2$ and $CoCO_3$ precipitates as well as some surface complexes. The experimental result herein suggests that Fe_3O_4@CD MNPs possess favorable application potential for the purification of Co(II)-bearing effluents in a wide pH range.

As shown in Fig. 3, the sorption percentage of 1-naphthol on Fe_3O_4@CD MNPs increases slowly from ~15% to ~25% as pH increases from 2.0 to 4.0, then increases sharply from ~25% to ~85% as pH increases from 4.0 to 9.0, and afterward decreases with increasing pH values. This phenomenon can be interpreted by the dissociation property of 1-naphthol in solution and the physicochemical property of Fe_3O_4@CD surface sites. As an ionizable aromatic compound, the 1-naphthol species is associated with its dissociated constant (pK_a) and the solution pH. Below its pK_a value of 9.34, 1-naphthol is present as nondissociated species in neutral form, and above this value 1-naphthol is in present as dissociated species in anionic form (inset in Fig. 3). At pH 2.0–4.0, the electrostatic repulsion between the nondissociated 1-naphthol species and the protonated Fe_3O_4@CD MNPs partly impedes the insertion of 1-naphthol into the hydrophobic cavity of the surface-coated β-CD molecules. In the pH range of 4.0–9.0, no obvious electrostatic repulsion is present between the neutral 1-naphthol species and the deprotonated Fe_3O_4@CD surfaces with negative charge. Consequently, the 1-naphthol molecules can be easily wrapped into the hydrophobic cavity of the surface-coated β-CD molecules, resulting in the sharp increase of sorption percentage. At pH > 9.0, the anionic 1-naphthol species are strongly repelled by the negatively charged Fe_3O_4@CD surfaces, leading to the reduction of sorption percentage in this pH range. In addition, the Fe_3O_4@CD MNPs are more hydrophilic at higher pH values. This variation trend will increase the affinity of their surface hydroxyl sites for water molecules via hydrogen-bond interaction. The surface-retained water molecules can serve as the binding centers for other water molecules, leading to the formation of water molecule clusters on Fe_3O_4@CD surfaces (Fontecha-Cámara, López-Ramón, Álvarez-Merino, & Moreno-Castilla, 2007). These clusters hinder the close approach of 1-naphthol molecules to the surfaces of Fe_3O_4@CD MNPs and correspondingly decrease the sorption percentage. Howsoever, the Fe_3O_4@CD MNPs still exhibit good removal performance toward 1-naphthol from both the acidic and alkaline solutions.

3.2.3. *Effect of ionic strength*

To disclose the underlying sequestration mechanisms, the sorption trends of Co(II) and 1-naphthol on Fe_3O_4@CD MNPs were investigated in 0.001, 0.01, 0.1 and 0.7 mol/L NaCl solutions, respectively. The tested ionic strength range herein covers the salinities of fresh water and seawater. As shown in Fig. 4A, the sorption of Co(II) is greatly affected by ionic strength variation at pH < 4.0, while no obvious difference can be observed at pH > 4.0. Herein, the ionic strength-dependent sorption trend at pH < 4.0 is attributed to the cation exchange/outer-sphere surface complexation (Yang et al., 2010). This deduction is supported by the fact that the sorption of Co(II) decreases with increasing ionic strength. At pH > 4.0, the ignorable effect of ionic strength suggests the occurrence of inner-sphere complexation. Furthermore, the formation of $Co(OH)_2$(s) precipitates may play an important role in the sequestration process of Co(II) by Fe_3O_4@CD MNPs at high alkaline pH. The ionic strength-independence of Co(II) sorption at pH > 4.0 suggests that Fe_3O_4@CD MNPs are feasible for the purification of Co(II)-bearing effluent under various salinity conditions.

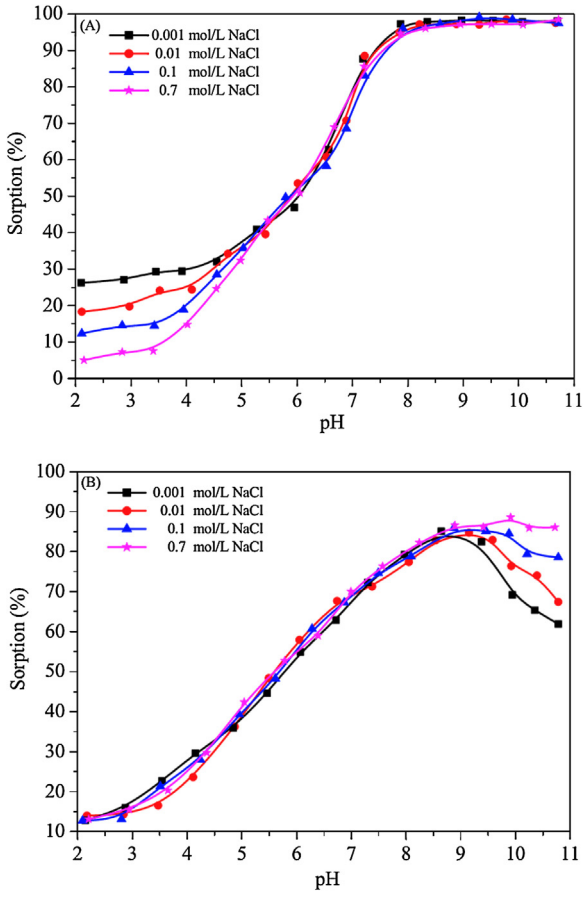

Fig. 4. Sorption of Co(II) (A) and 1-naphthol (B) on Fe_3O_4@CD MNPs as a function of ionic strength. T = 293 K, m/V = 0.5 g/L, $C_{Co(II)}$ = 10 mg/L, $C_{1\text{-naphthol}}$ = 50 mg/L.

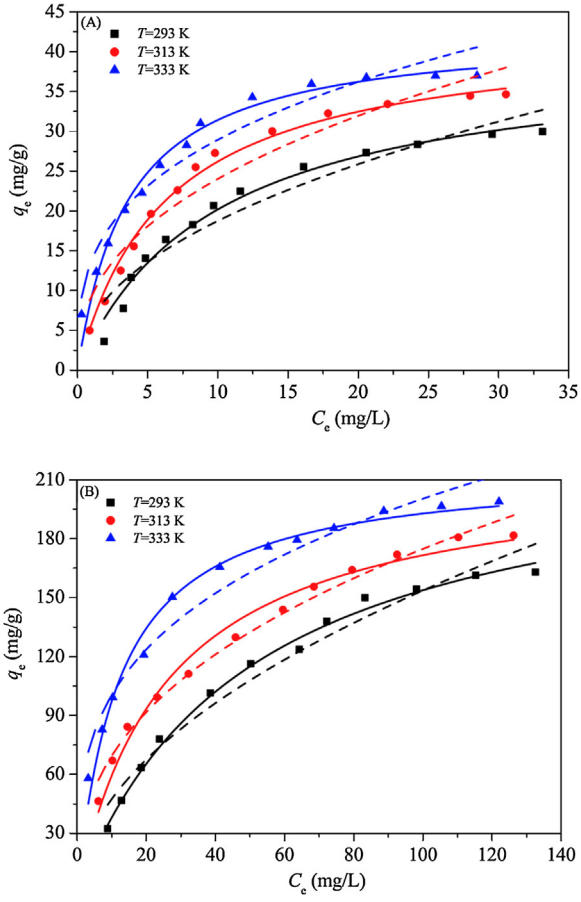

Fig. 5. Sorption isotherms and model fittings of Co(II) (A) and 1-naphthol (B) on Fe_3O_4@CD MNPs. Symbols represent the sorption isotherms, solid lines represent the fitting of Langmuir model and dash lines represent the fitting of Freundlich model. pH = 6.5, m/V = 0.5 g/L, I = 0.01 mol/L NaCl.

As shown in Fig. 4B, the sorption of 1-naphthol is not influenced by ionic strength variation at pH < 9.0, while increases with increasing ionic strength at pH > 9.0. As mentioned above, 1-naphthol is present as nondissociated species in neutral form at pH < 9.0 (see the inset in Fig. 3). Hence, its aqueous solubility and activity coefficient are not affected by ionic strength variation due to the low coordination ability of electronic ions with the nondissociated species (Chen, Chen, & Zhu, 2008; Yang, Wu, Jing, & Zhu, 2008). In view of this, the ionic strength-independent sorption at pH < 9.0 arises from the inclusion reaction due to hydrophobic effect. At pH > 9.0, repulsive electrostatic interaction occurs between the negatively charged Fe_3O_4@CD MNPs and the dissociated 1-naphthol species in anionic form. At higher ionic strength, the electrostatic repulsion between these two negatively charged moieties can be effectively reduced due to the screening effect on the surface charge. This variation trend will create a favorable electrostatic environment for the close approach of 1-naphthol to Fe_3O_4@CD MNPs. In addition, the increase of ionic strength is expected to reduce the solubility of 1-naphthol due to the "salting out" effect (i.e., the strong coordination ability of electronic ions with the dissociated species), which enhances the hydrophobic interaction and thus increases the sorption percentage. In a previous study, an increase in KCl concentration was reported to increase the uptake of herbicide diuron on activated carbon fiber (Fontecha-Cámara et al., 2007). In contrast, the sorption affinities of nonionic aromatic compounds to carbon nanotubes were not influenced by ionic strength variation (Chen et al., 2008; Pan, & Xing, 2008). The differences between our study and the literatures are caused by various factors such as the physiochemical properties of adsorbates, the surface properties of solid particles as well as the type and concentration range of electrolyte solution.

3.2.4. Sorption isotherms

Fig. 5A and B illustrates the sorption isotherms of Co(II) and 1-naphthol on Fe_3O_4@CD MNPs at three different temperatures (viz. 293, 313 and 333 K). Both the sorption amounts of Co(II) and 1-naphthol increase with increasing equilibrium concentration in solution. Herein, higher concentrations of Co(II) and 1-naphthol can provide greater driving force for overcoming the mass transfer limitation between the aqueous phase and the bulk phase of Fe_3O_4@CD MNPs. In addition, higher concentrations can enhance the collisions between Co(II)/1-naphthol and Fe_3O_4@CD MNPs, resulting in the higher sorption amounts (Rathinam, Maharshi, Janardhanan, Jonnalagadda, & Nair, 2010; Vimala & Das, 2009). Note that both the sorption isotherms of Co(II) and 1-naphthol reveal the typical L shape. This phenomenon eliminates the occurrence of surface (co)precipitation, which is expected to induce an exponential increase of sorption amount with increasing equilibrium concentration. For both Co(II) and 1-naphthol, the sorption isotherm is the highest at 333 K and is the lowest at 293 K, suggesting the occurrence of endothermic reaction for Co(II) and 1-naphthol binding on Fe_3O_4@CD MNPs.

To deduce the underlying sorption mechanisms, the sorption isotherms are simulated with Langmuir $\left(q_e = bq_{max}C_e/(1 + bC_e)\right)$ and Freundlich ($q_e = K_F C_e^{\,n}$) models. In the equations, C_e is the residual concentration of adsorbates in solution (mg/L); q_e is the sorption amount after equilibrium (mg/g); q_{max} is the maximum sorption

amount at complete monolayer coverage (mg/g); b is a parameter that relates to the sorption heat (L/mg); K_F represents the sorption capacity when the equilibrium concentration of adsorbates equals to 1 ($mg^{1-n}/g\,L^n$) and n represents the sorption dependence degree. The parameters derived from the model fittings are listed in Table S1. One can see from the R^2 values that Langmuir model simulates the experimental data better than Freundlich model. This result implies that chemisorption is the principal driving force for Co(II) and 1-naphthol binding on Fe_3O_4@CD MNPs (Zhou, Nie, Branford-White, He, & Zhu, 2009). The small n values (<1) suggest that a nonlinear sorption process occurs on Fe_3O_4@CD MNPs. Overall, the derived parameters indicate that the sorption of Co(II) and 1-naphthol on Fe_3O_4@CD MNPs is a favorable and chemisorption process. Herein, the maximum sorption capacities (i.e., q_{max}) of Fe_3O_4@CD MNPs toward Co(II) and 1-naphthol are carefully compared with other adsorbents to further check the potential of using this material in effluent purification. From Tables S2 and S3, one can see that the q_{max} values of Co(II) and 1-naphthol on Fe_3O_4@CD MNPs are higher than a series of adsorbent materials. In view of this, Fe_3O_4@CD MNPs can be potentially used in wastewater disposal with favorable environmental and economic benefits. More detailed information on the comparation of maximum sorption capacities between Fe_3O_4@CD MNPs and other materials is described in the Supporting information. The thermodynamic parameters (ΔH°, ΔS°, and ΔG°) (Table S4) derived from the sorption isotherms suggest that the sorption processes of Co(II) and 1-naphthol on Fe_3O_4@CD MNPs are spontaneous and endothermic. Detailed information on the thermodynamic analysis is described in the Supporting information.

3.3. Binary-solute sorption systems

3.3.1. Effect of 1-naphthol concentration on Co(II) sorption

Fig. 6A shows the sorption of Co(II) on Fe_3O_4@CD MNPs as a function of initial 1-naphthol concentration. It is clear that Co(II) sorption percentage increases with increasing 1-naphthol concentration at $C_{1\text{-naphthol}} < 80$ mg/L, while decreases with increasing 1-naphthol concentration at $C_{1\text{-naphthol}} > 80$ mg/L. In general, the sorption of heavy metal ions on material surfaces can be influenced by the coexisting organic components through various interaction mechanisms. On one hand, the simultaneous organic matter can join the solid surface sites and the metal ions in solution. This interaction is expected to enhance the sorption of metal ions via the formation of ternary surface complexes (Polubesova, Zadaka, Groisman, & Nir, 2006). On the other hand, the coexistent organic matter can compete with metal ions for surface binding sites and also complete with surface binding sites for dissolved metal ions (MacKay, & Canterbury, 2005; Wang, Jia, Sun, Zhu, & Zhou, 2008). These two interactions will reduce the sorption of metal ions on solid surfaces. Moreover, the dissociation of organic matter can change the solution pH, which will further influence the physicochemical properties of solid particles, the species of metal ions and accordingly the sorption of metal ions (Zhou, Wang, Cang, Hao, & Luo, 2004). As discussed above, 1-naphthol is captured by incorporating the hydrophobic phenyl groups into the cavity of surface-coated β-CD molecules, keeping the hydrophilic phenolic hydroxyl groups outside the cavity. As the initial concentration of 1-naphthol increases, more phenolic hydroxyl groups are available as active sites to form complexes with Co(II) ions, resulting in the increase of Co(II) sorption percentage. This experimental phenomenon also points to the formation of type B ternary complexes, i.e., the "ligand-bridging" Fe_3O_4@CD-naphthol-Co(II). However, at higher 1-naphthol concentration, the cavity numbers of the β-CD molecules are not adequate for the incorporation of 1-naphthol. The remaining 1-naphthol forms complexes with Co(II) in solution and thereby competitively diminishes the sorption percentage of

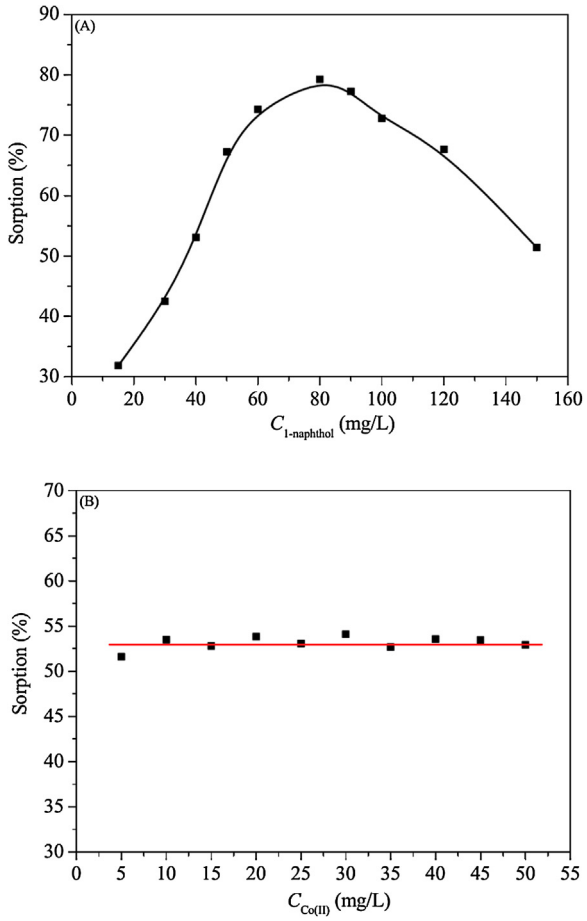

Fig. 6. Effect of initial 1-naphthol and Co(II) concentration on the sorption of Co(II) (A) and 1-naphthol (B) on Fe_3O_4@CD MNPs. $T = 293$ K, pH = 6.5, $m/V = 0.5$ g/L, $I = 0.01$ mol/L NaCl.

Co(II) on Fe_3O_4@CD MNPs. A previous study reported that the acid blue 25 dye enhanced the sorption of Zn(II), Ni(II) and Cd(II) on $Ca(PO_3)_2$-modified carbon (Tovar-Gómez et al., 2012). Similarly, tetracycline increased the sorption of Cu(II) on montmorillonite due to the stronger affinity of tetracycline-Cu(II) complexes to montmorillonite (Wang et al., 2008). However, some dissolved organic matters significantly reduced the sorption capacities of Cd(II), Zn(II) and Cu(II) on soils (Ashworth, & Alloway, 2007; Wong, Li, Zhou, & Selvam, 2007). The foregoing similarities and differences are attributed to various factors such as the surface properties of solid particles, the chemical species of metal ions, the nature of organic matters as well as the solution chemistry conditions.

3.3.2. Effect of Co(II) concentration on 1-naphthol sorption

Fig. 6B shows the sorption of 1-naphthol on Fe_3O_4@CD MNPs as a function of initial Co(II) concentration in solution. One can see that the variation of initial Co(II) concentration exhibits no obvious influence on 1-naphthol sorption. Generally, the coexisting metal ions can bridge the organic matters and the solid surface sites, compress the electric double layer, neutralize the negative charges of organic matters and thereby influence the sequestration of organic matters on solid particles (Hyung, & Kim, 2008; Lu, & Su, 2007). However, the experimental phenomenon herein suggests that the Co(II) ions in solution are incapable to obstruct the inclusion of 1-naphthol into the β-CD cavities via hydrophobic effect. This result also eliminates the potential formation of type A ternary complexes, i.e., the "metal-bridging" Fe_3O_4@CD-Co(II)-naphthol. If Co(II) and 1-naphthol were simultaneously retained on Fe_3O_4@CD

MNPs to form type A ternary complexes, the sorption percentage of 1-naphthol would increase with increasing Co(II) concentration. Alternatively, one may deduce the formation of type B ternary complexes, i.e., the "ligand-bridging" Fe_3O_4@CD-naphthol-Co(II). By integrating the effect of 1-naphthol concentration on Co(II) sorption (Fig. 6A), one can conclude that Fe_3O_4@CD MNPs can be used for the simultaneous removal of Co(II) and 1-naphthol in a wide concentration range.

3.3.3. *Effect of addition sequence*

The real aquatic system is a complicated and multicomponent environmental medium. The addition sequences of heavy metal ions, organic pollutants and the solid materials significantly influence their sorption trends and species distribution (Floroiu, Davis, & Torrents, 2001). In view of this, the sorption behaviors of Co(II) and 1-naphthol on Fe_3O_4@CD MNPs were investigated as a function of solution pH for the following four sequences: (1) the Fe_3O_4@CD MNPs, Co(II) and 1-naphthol stock solutions were simultaneously added into the vials and the resulting mixtures were gently oscillated for 24 h (denoted as batch 1); (2) the Fe_3O_4@CD MNPs and Co(II) stock solution were pre-equilibrated for 24 h before the addition of 1-naphthol stock solution (denoted as batch 2); (3) the Fe_3O_4@CD MNPs and 1-naphthol stock solution were pre-equilibrated for 24 h before the addition of Co(II) stock solution (denoted as batch 3); and (4) the Co(II) and 1-naphthol stock solutions were pre-equilibrated for 24 h before the addition of Fe_3O_4@CD MNPs (denoted as batch 4). The test herein is of great significance to check the reversibility of the sorption process and assess the application potential of Fe_3O_4@CD MNPs in wastewater disposal.

One can see from Fig. 7A that the sorption of Co(II) on Fe_3O_4@CD MNPs exhibits discrepant trends for the four different addition sequences. Specifically, the sorption percentage shows an order of batch 1 ≈ batch 3 > batch 2 > batch 4. For batch 1 and batch 3, the Co(II) ions can be sequestrated on the surface hydroxyl sites of Fe_3O_4@CD MNPs and the phenolic hydroxyl groups of 1-naphthol outside the cavity of surface-coated β-CD moieties. For batch 2, the subsequently added 1-naphthol is expected to desorb some Co(II) ions that have been pre-adsorbed on the surfaces of Fe_3O_4@CD MNPs. The formation of 1-naphthol-Co(II) complexes in solution would lead to the slight decline of Co(II) sorption percentage. For batch 4, the Co(II) in solution is present in the form of soluble 1-naphthol-Co(II) complexes instead of the hydrated ions. Compared with the hydrated Co(II) ions, the soluble 1-naphthol-Co(II) complexes with hydrophobic phenyl groups are more difficult to bind on the hydrophilic surface sites of Fe_3O_4@CD MNPs. This is the tentative interpretation for the decrease of Co(II) sorption percentage.

As shown in Fig. 7B, the sorption percentage of 1-naphthol on Fe_3O_4@CD MNPs exhibits an order of batch 1 ≈ batch 3 ≈ batch 4 > batch 2. For batch 1, batch 3 and batch 4, the hydrophobic phenyl groups of 1-naphthol can easily incorporate into the hydrophobic cavity of surface-coated β-CD molecules, leading to similar 1-naphthol sorption trends in these three systems. For batch 2, the surface hydroxyl sites of Fe_3O_4@CD MNPs have been occupied by the Co(II) ions before the addition of 1-naphthol. The hydrophilic environment caused by the hydration layer of adsorbed Co(II) ions is unfavorable for the sequestration of hydrophobic 1-naphthol. In addition, the surface-adsorbed Co(II) ions may reduce the size of the β-CD cylindrical cavity, which will disturb the host–guest consistency and further hinder the inclusion of hydrophobic 1-naphthol. Hence, the sorption percentage of 1-naphthol on Fe_3O_4@CD MNPs in batch 2 is lower than those in the other three addition sequences.

According to the above-mentioned experimental results and analysis, it is clear that the addition sequence of different components can influence the removal performance of Fe_3O_4@CD MNPs. Herein, the sorption percentages of both Co(II) and 1-naphthol in batch 1 and batch 3 are higher than those in batch 2 and batch 4. To improve the removal efficiency of Fe_3O_4@CD MNPs toward Co(II) and 1-naphthol, one should mingle the Fe_3O_4@CD MNPs, Co(II) and 1-naphthol stock solutions simultaneously or premix the Fe_3O_4@CD MNPs and 1-naphthol stock solution before the addition of Co(II) stock solution.

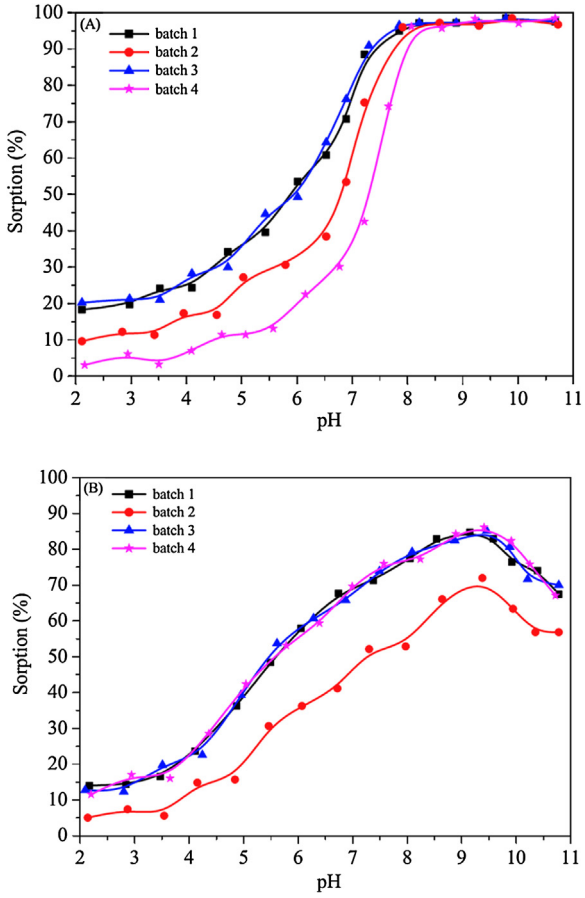

Fig. 7. Effect of addition sequence on Co(II) (A) and 1-naphthol (B) sorption on Fe_3O_4@CD MNPs. T = 293 K, m/V = 0.5 g/L, $C_{Co(II)}$ = 10 mg/L, $C_{1\text{-naphthol}}$ = 50 mg/L, I = 0.01 mol/L NaCl.

3.4. *Simulated effluent purification*

Owing to the heterogeneity and complexity of aquatic environment, the removal performance of Fe_3O_4@CD MNPs toward a simulated effluent was further tested to corroborate the research findings obtained from the foregoing experiments. To better reflect the heterogeneous water system, the simulated effluent consists of 10 mg/L of Cd(II), 10 mg/L of Co(II), 5 mg/L of phosphate, 5 mg/L of As(V), 30 mg/L of methylene blue (MB), 50 mg/L 1-naphthol, 10 mg/L of humic acid (HA) and 0.01 mol/L NaCl electrolyte solution. Typical experiment was performed by adding 200 mL of the simulated effluent into a 500 mL beaker. The subsequent procedure was conducted at pH 6.5 via a similar approach as that in batch experiments. The analysis results show that the removal percentages of Fe_3O_4@CD MNPs toward Cd(II), Co(II), phosphate, As(V), MB, 1-naphthol and HA are 52%, 57%, 45%, 42%, 50%, 59% and 41%, respectively. Note that Fe_3O_4@CD MNPs still exhibit good removal performance toward Co(II) and 1-naphthol in the simulated effluent. The results herein can provide more accurate experimental parameters for evaluate the application potential of Fe_3O_4@CD MNPs in the actual wastewater treatment.

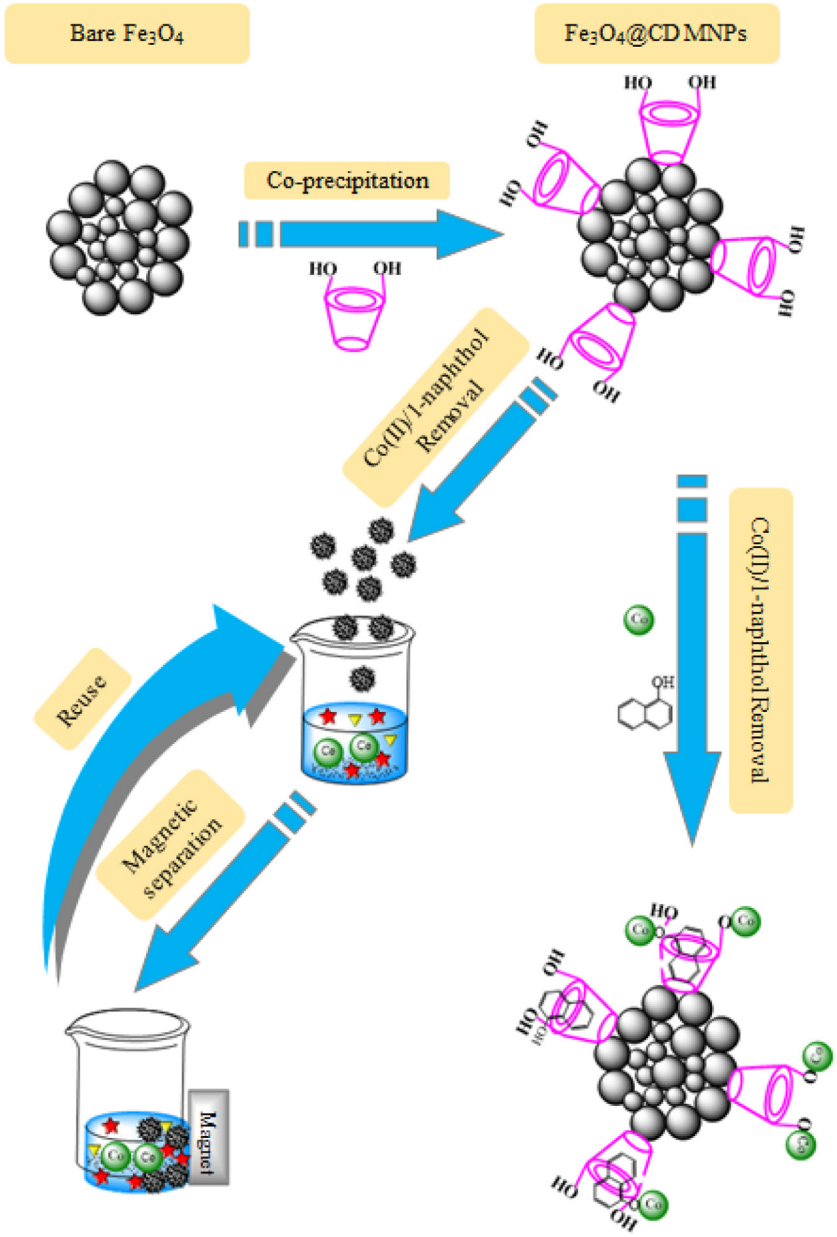

Fig. 8. Schematic illustration for the simultaneous removal of Co(II) and 1-naphthol by Fe_3O_4@CD MNPs.

4. Conclusions

The present study reports the preparation of core–shell structured Fe_3O_4@CD MNPs by using a simple chemical co-precipitation method. The raw materials (i.e., iron salts and β-CD) used for the synthesis of Fe_3O_4@CD MNPs are abundant and harmless to the environment. Consequently, the as-prepared Fe_3O_4@CD MNPs are low-cost and eco-friendly. The high dispersion and plentiful binding sites of Fe_3O_4@CD MNPs contribute to their favorable removal performance toward Co(II) and 1-naphthol. The experimental results derived from the binary-solute system and the simulated effluent suggest that Fe_3O_4@CD MNPs can support the simultaneous removal of Co(II) and 1-naphthol via the binding of Co(II) on the external surface sites and the incorporation of 1-naphthol into the hydrophobic cavity of surface-coated β-CD molecules (Fig. 8). According to the disparate sorption trends for different addition sequences, one should adopt appropriate addition sequence to improve the removal efficiency of Fe_3O_4@CD MNPs. By considering the abundant and low-cost raw materials, simple synthesis approach, environmental friendliness, favorable removal efficiency and convenient separation performance, Fe_3O_4@CD MNPs can exhibit great application potential in environmental protection field.

Acknowledgements

Financial support from the National Natural Science Foundation of China (No. 41203086), the Jiangsu Provincial Key Laboratory of Radiation Medicine and Protection and the Priority Academic Program Development of Jiangsu Higher Education Institutions are acknowledged.

Appendix A. Supplementary data

Supplementary data associated with this article can be found, in the online version, at http://dx.doi.org/10.1016/j.carbpol.2014.08.072.

References

Al-Qunaibit, M. H., Mekhemer, W. K., & Zaghloul, A. A. (2005). The adsorption of Cu(II) ions on bentonite-a kinetic study. *Journal of Colloid and Interface Science*, *283*, 316–321.

Ashworth, D. J., & Alloway, B. J. (2007). Complexation of copper by sewage sludge-derived dissolved organic matter: Effects on soil sorption behaviour and plant uptake. *Water, Air, & Soil Pollution*, *182*, 187–196.

Badruddoza, A. Z. M., Tay, A. S. H., Tan, P. Y., Hidajat, K., & Uddin, M. S. (2011). Carboxymethyl-β-cyclodextrin conjugated magnetic nanoparticles as nano-adsorbents for removal of copper ions: Synthesis and adsorption studies. *Journal of Hazardous Materials*, *185*, 1177–1186.

Bhattacharyya, K. G., & Gupta, S. S. (2008). Influence of acid activation on adsorption of Ni(II) and Cu(II) on montmorillonite: Kinetic and thermodynamic study. *Chemical Engineering Journal*, *136*, 1–13.

Chen, A. W., Zeng, G. M., Chen, G. Q., Hua, X. J., Yan, M., Guan, S., et al. (2012). Novel thiourea-modified magnetic ion-imprinted chitosan/TiO_2 composite for simultaneous removal of cadmium and 2,4-dichlorophenol. *Chemical Engineering Journal*, *191*, 85–94.

Chen, J., Chen, W., & Zhu, D. Q. (2008). Adsorption of nonionic aromatic compounds to single-walled carbon nanotubes: Effects of aqueous solution chemistry. *Environmental Science & Technology*, *42*, 7225–7230.

Chen, Q. C., Zhang, R., Wang, J., Li, L., & Guo, X. H. (2012). Spherical particles of α-β- and γ-cyclodextrin polymers and their capability for phenol removal. *Materials Letters*, *79*, 156–158.

Chen, Y., & Liu, Y. (2010). Cyclodextrin-based bioactive supramolecular assemblies. *Chemical Society Reviews*, *39*, 495–505.

del Valle, E. M. M. (2004). Cyclodextrins and their uses: A review. *Process Biochemistry*, *39*, 1033–1046.

Diaz-Flores, P. E., López-Urías, F., Terrones, M., & Rangel-Mendez, J. R. (2009). Simultaneous adsorption of Cd^{2+} and phenol on modified N-doped carbon nanotubes: Experimental and DFT studies. *Journal of Colloid and Interface Science*, *334*, 124–131.

Floroiu, R. M., Davis, A. P., & Torrents, A. (2001). Cadmium adsorption on aluminum oxide in the presence of polyacrylic acid. *Environmental Science & Technology*, *35*, 348–353.

Fontecha-Cámara, M. A., López-Ramón, M. V., Álvarez-Merino, M. A., & Moreno-Castilla, C. (2007). Effect of surface chemistry, solution pH, and ionic strength on the removal of herbicides diuron and amitrole from water by an activated carbon fiber. *Langmuir*, *23*, 1242–1247.

Fuhrer, R., Herrmann, I. K., Athanassiou, E. K., Grass, R. N., & Stark, W. J. (2011). Immobilized β-cyclodextrin on surface-modified carbon-coated cobalt nanomagnets: Reversible organic contaminant adsorption and enrichment from water. *Langmuir*, *27*, 1924–1929.

Gustafsson, J. P. (2011). *Visual MINTEQ ver. 3.0*. Stockholm, Sweden: Department of Land and Water Resources Engineering, KTH (Royal Institute of Technology). Available at http://www2.lwr.kth.se/English/OurSoftware/vminteq/index.htm

Hyung, H., & Kim, J. H. (2008). Natural organic matter (NOM) adsorption to multi-walled carbon nanotubes: Effect of NOM characteristics and water quality parameters. *Environmental Science & Technology*, *42*, 4416–4421.

Jović-Jovičić, N., Milutinović-Nikolić, A., Banković, P., Mojović, Z., Žunić, M., Gržetić, I., et al. (2010). Organo-inorganic bentonite for simultaneous adsorption of acid orange 10 and lead ions. *Applied Clay Science*, *47*, 452–456.

Liu, J. F., Zhao, Z. S., & Jiang, G. B. (2008). Coating Fe_3O_4 magnetic nanoparticles with humic acid for high efficient removal of heavy metals in water. *Environmental Science & Technology*, *42*, 6949–6954.

Liu, Q. T., Diamond, M. L., Gingrich, S. E., Ondov, J. M., Maciejczyk, P., & Stern, G. A. (2003). Accumulation of metals, trace elements and semi-volatile organic compounds on exterior window surfaces in Baltimore. *Environmental Pollution*, *122*, 51–61.

Loftsson, T., & Brewster, M. E. (2011). Pharmaceutical applications of cyclodextrins: Effects on drug permeation through biological membranes. *Journal of Pharmacy and Pharmacology*, *63*, 1119–1135.

Lu, C. Y., & Su, F. S. (2007). Adsorption of natural organic matter by carbon nanotubes. *Separation and Purification Technology*, *58*, 113–121.

Ma, J. W., Wang, F. Y., Huang, Z. H., & Wang, H. (2010). Simultaneous removal of 2,4-dichlorophenol and Cd from soils by electrokinetic remediation combined with activated bamboo charcoal. *Journal of Hazardous Materials*, *176*, 715–720.

MacKay, A. A., & Canterbury, B. (2005). Oxytetracycline sorption to organic matter by metal-bridging. *Journal of Environmental Quality*, *34*, 1964–1971.

Maturi, K., & Reddy, K. R. (2006). Simultaneous removal of organic compounds and heavy metals from soils by electrokinetic remediation with a modified cyclodextrin. *Chemosphere*, *63*, 1022–1031.

Morin-Crini, N., & Crini, G. (2013). Environmental applications of water-insoluble β-cyclodextrin-epichlorohydrin polymers. *Progress in Polymer Science*, *38*, 344–368.

Oleszczuk, P., Pan, B., & Xing, B. S. (2009). Adsorption and desorption of oxytetracycline and carbamazepine by multiwalled carbon nanotubes. *Environmental Science & Technology*, *43*, 9167–9173.

Pan, B., & Xing, B. S. (2008). Adsorption mechanisms of organic chemicals on carbon nanotubes. *Environmental Science & Technology*, *42*, 9005–9013.

Polubesova, T., Zadaka, D., Groisman, L., & Nir, S. (2006). Water remediation by micelle-clay system: Case study for tetracycline and sulfonamide antibiotics. *Water Research*, *40*, 2369–2374.

Rathinam, A., Maharshi, B., Janardhanan, S. K., Jonnalagadda, R. R., & Nair, B. U. (2010). Biosorption of cadmium metal ion from simulated wastewaters using Hypnea valentiae biomass: A kinetic and thermodynamic study. *Bioresource Technology*, *101*, 1466–1470.

Shen, H. Y., Pan, S. D., Zhang, Y., Huang, X. L., & Gong, H. X. (2012). A new insight on the adsorption mechanism of amino-functionalized nano-Fe_3O_4 magnetic polymers in Cu(II), Cr(VI) co-existing water system. *Chemical Engineering Journal*, *183*, 180–191.

Singh, S., Barick, K. C., & Bahadur, D. (2013). Fe_3O_4 embedded ZnO nanocomposites for the removal of toxic metal ions, organic dyes and bacterial pathogens. *Journal of Material Chemistry A*, *1*, 3325–3333.

Tovar-Gómez, R., Rivera-Ramírez, D. A., Hernández-Montoya, V., Bonilla-Petriciolet, A., Durán-Valle, C. J., & Montes-Morán, M. A. (2012). Synergic adsorption in the simultaneous removal of acid blue 25 and heavy metals from water using a $Ca(PO_3)_2$-modified carbon. *Journal of Hazardous Materials*, *199–200*, 290–300.

Vimala, R., & Das, N. (2009). Biosorption of cadmium(II) and lead(II) from aqueous solutions using mushrooms: A comparative study. *Journal of Hazardous Materials*, *168*, 376–382.

Visa, M., Bogatu, C., & Duta, A. (2010). Simultaneous adsorption of dyes and heavy metals from multicomponent solutions using fly ash. *Applied Surface Science*, *256*, 5486–5491.

Wang, G. H., Zhou, Y. M., Wang, X. G., Chai, X. J., Huang, L., & Deng, N. S. (2010). Simultaneous removal of phenanthrene and lead from artificially contaminated soils with glycine-β-cyclodextrin. *Journal of Hazardous Materials*, *184*, 690–695.

Wang, S. W., Dong, Y. H., He, M. L., Chen, L., & Yu, X. J. (2009). Characterization of GMZ bentonite and its application in the adsorption of Pb(II) from aqueous solutions. *Applied Clay Science*, *43*, 164–171.

Wang, X. L., Tao, S., & Xing, B. S. (2009). Sorption and competition of aromatic compounds and humic acid on multiwalled carbon nanotubes. *Environmental Science & Technology*, *43*, 6214–6219.

Wang, Y. J., Jia, D. A., Sun, R. J., Zhu, H. W., & Zhou, D. M. (2008). Adsorption and cosorption of tetracycline and copper(II) on montmorillonite as affected by solution pH. *Environmental Science & Technology*, *42*, 3254–3259.

Wong, J. W. C., Li, K. L., Zhou, L. X., & Selvam, A. (2007). The sorption of Cd ad Zn by different soils in the presence of dissolved organic matter from sludge. *Geoderma*, *137*, 310–317.

Yang, K., Wu, W. H., Jing, Q. F., & Zhu, L. Z. (2008). Aqueous adsorption of aniline, phenol and their substitutes by multi-walled carbon nanotubes. *Environmental Science & Technology*, *42*, 7931–7936.

Yang, S. T., Zhao, D. L., Zhang, H., Lu, S. S., Chen, L., & Yu, X. J. (2010). Impact of environmental conditions on the sorption behavior of Pb(II) in Na-bentonite suspensions. *Journal of Hazardous Materials*, *183*, 632–640.

Yang, S. T., Zong, P. F., Ren, X. M., Wang, Q., & Wang, X. K. (2012). Rapid and high-efficient preconcentration of Eu(III) by core–shell structured Fe_3O_4@humic acid magnetic nanoparticles. *ACS Applied Materials & Interfaces*, *4*, 6891–6900.

Zhang, S. X., Niu, H. Y., Cai, Y. Q., Zhao, X. L., & Shi, Y. L. (2010). Arsenite and arsenate adsorption on coprecipitated bimetal oxide magnetic nanomaterials: $MnFe_2O_4$ and $CoFe_2O_4$. *Chemical Engineering Journal*, *158*, 599–607.

Zhou, D. M., Wang, Y. J., Cang, L., Hao, X. Z., & Luo, X. S. (2004). Adsorption and cosorption of cadmium and glyphosate on two soils with different characteristics. *Chemosphere*, *57*, 1237–1244.

Zhou, Y. T., Nie, H. L., Branford-White, C., He, Z. Y., & Zhu, L. M. (2009). Removal of Cu^{2+} from aqueous solution by chitosan-coated magnetic nanoparticles modified with α-ketoglutaric acid. *Journal of Colloid and Interface Science*, *330*, 29–37.

Zhu, H. X., Jia, S. R., Wan, T., Jia, Y. Y., Yang, H. J., Li, J., et al. (2011). Biosynthesis of spherical Fe_3O_4/bacterial cellulose nanocomposites as adsorbents for heavy metal ions. *Carbohydrate Polymers*, *86*, 1558–1564.